Inter*net* Electronic Journal*

Nanociencia et Moletrónica

Julio 2010, Vol. 8, N°1, pp. 1473 - 1488

Micro-structural changes in the amorphous Fe-based alloy 2605S3A prior to crystallization.

Part 2. Positron annihilation lifetime spectroscopy

A. López-Morales[1], A. Cabral-Prieto[2], F. García-Santibáñez[1], J. Ramírez[2], J. López-Monroy[2], J. Orozco-Velazco[1]

[1] Laboratorio de Física de Materiales, Facultad de Ciencias,
Universidad Autónoma del Estado de México,
El Cerillo Piedras Blancas, Toluca, Estado de México, ***México***
[2] Instituto Nacional de Investigaciones Nucleares), Ocoyoacac, Estado de México, ***México****.*

recibido: 16.11.09 revisado: 22.04.10 publicado: 31.07.10

Citation of the article;
A. López-Morales, A. Cabral-Prieto, F. García-Santibáñez, J. Ramírez, J. López-Monroy, J. Orozco-Velazco, Micro-structural changes in the amorphous Fe-based alloy 2605S3A prior to crystallization. Part 2: Positron annihilation lifetime spectroscopy,
Int. Electron J. Nanoc. Moletrón, 2010, Vol. 8, N°1, pp 1473-1488

Micro-structural changes in the amorphous Fe-based alloy 2605S3A prior to crystallization.

Part 2. Positron annihilation lifetime spectroscopy

A. López-Morales[1], A. Cabral-Prieto[2], F. García-Santibáñez[1], J. Ramírez[2], J. López-Monroy[2], J. Orozco-Velazco[1]

[1] Laboratorio de Física de Materiales, Facultad de Ciencias,
Universidad Autónoma del Estado de México,
El Cerillo Piedras Blancas, Toluca, Estado de México, ***México***
[2] Instituto Nacional de Investigaciones Nucleares), Ocoyoacac, Estado de México, ***México****.*

recibido: 16.11.09 revisado: 22.04.10 publicado: 31.07.10

Internet Electron. J. Nanoc. Moletrón., 2010, Vol.8 , N° 1, pp 1473-1488

Abstract

Clusters of 24 and 32 mono-vacancies in the amorphous and crystalline states of the 2605S3A alloy, respectively, having 0.44 nm mean radii and a mean relative concentration of clusters of $C = 1.68x10^{-8}$ atoms^{-1} between these states were measured by the positron annihilation process. Slight variations of size and concentration of these clusters were the source of micro-structural changes in the alloy as reflected in its mechanical and magnetic properties and at the phase transitions. For instance, the alloy treated at 634K became slightly brittle having the smallest clusters of 0.41 nm radii. The alloy then treated at 672K and undertook a magnetic reorientation with $\alpha = 4$ having the largest defects of ~0.46 nm radii. These results are analyzed in terms of the micro-structural changes occurring in the alloy making use of positron annihilation lifetime spectroscopy (PALS) and results presented in the Part I of this work.
Keywords: crystalline defects, positron annihilation lifetime spectroscopy

Resumen

Cúmulos de 24 y 32 monovacancias en los estados amorfo y cristalino, de la aleación 2605S3A. Ellos tienen radios medios de 0.44nm y una concentración media relativa de cúmulos de $C = 1.68x10^{-8}$ átomos^{-1} para ambos estados amorfo y cristalino, que fueron medidos por el proceso de aniquilación de positrones. Las ligeras variaciones del tamaño y la concentración de estos cúmulos fueron la fuente de cambios microestructurales en la aleación, como se reflejaron en sus propiedades mecánicas y magnéticas y en las transiciones de fase. Estos resultados son analizados en términos de los cambios microestructurales que ocurrieron en la aleación haciendo uso de espectroscopia del tiempo de vida de aniquilación del positrón (PALS) y de los resultados presentados en la Parte I de este trabajo

1. Introduction

Since the first developments on inter-metallic compounds in 1946 [1], several scientific and technological interests have remained ever since. One of these interests is connected with the production of amorphous alloys with soft magnetic properties, by which the chemical composition of the alloys has thoroughly been modified and investigated. There have emerged from this effort not only several techniques to produce them but also a great variety of alloys with different elemental compositions and magnetic properties; which, in addition, have been widely used in electromagnetic devices working at low or high frequencies [2] and more restricted in high power transformers [3]. The technological applications of these amorphous alloys have been restricted to low-working temperatures because of their mechanical properties, which become brittle in the crystalline state. This mechanical handicap appears either in thin sheets or bulk amorphous alloys, and whether this handicap can be subdued is a matter of continuous research [4, 5]. Particularly, the ductility of the Fe-based amorphous alloys slowly decreases while being transformed from the amorphous to the crystalline state [5, 6]. Such a loss of ductility is generally accepted to be due to the presence of different crystalline phases from pure Fe in the crystalline state [7]. Another source contributing to such a loss of ductility is the presence of crystalline defects, which may vary in size or in concentration prior to or throughout the phase transitions. Such variations in size and/or concentration of defects have been reported to produce other property changes in the alloy, like changes in the magnetic properties [8]. Thus, the brittleness problem of these Fe-based amorphous alloys greatly depends on the elemental nature of the alloy, the presence of crystalline phases other than pure Fe and on mass and/or volumetric defects and their concentration, among other sources.

A well-established technique to study mass and volumetric defects in metals is Positron Annihilation Lifetime Spectroscopy (PALS) [9, 10]. This technique is based on injecting positrons into the metal. These positrons usually come from a β^+ emitter, such as ^{22}Na, which decays to ^{22}Ne as a result of its nuclear decay process. The initial positron energy of ~ 500 keV is lost within the metal in fractions of ps because of inelastic interactions with the atoms of the metal. Once the positrons have lost most of their energy and are thermalized, a diffusive process starts, being characteristic for each metal; this process is over when the positron is bound to an electron from the metal and they annihilate each other. The positron-electron pairs so created annihilate with characteristic lifetimes depending on the electronic properties, mass and open-volume defects of the metal. From the positron birth, detected with the de-excitation 1.27 MeV photons, simultaneously emitted with the positron from the new ^{22}Ne atom, up to the detection of the annihilation pair 0.511 KeV photons, an elapsing time from 0.125 to 140 ns can be measured [9, 10]. In particular, it is possible to characterize different mass or volumetric defects in metals or

alloys with PALS because there exists a neat difference between the positron annihilation lifetimes in a defect-free metal and a non-defect-free metal [11].

Thus, in the present paper the Fe-based amorphous alloy 26053SA was thermally treated from 325 to 810K, where the mechanical properties were studied by measuring the Vickers micro-hardness number, H_V. The corresponding micro-structural changes occurring in the alloy were studied by using Mössbauer spectroscopy (MS) [12], X-Ray Diffraction (XRD) and PALS.

2. Experimental

We analyze the Fe-based amorphous alloy 2605S3A that was obtained from Metglass Inc. Co., USA as a gift from J. Jordan and Dr. Hasegawa. The alloy consists of a long sheet 20 μm thick, 100 cm long x 5 cm wide.

For all the preceding measurements, foils of 2 cm long x 2 cm wide were used. The positron annihilation lifetime spectra were recorded by utilizing a fast-fast gamma ray coincidence system with a resolution function system of 0.29 ns. The resulting spectra were analyzed with the Positron program [13] and a homemade program. For these measurements, the sample was prepared as follows: micro-drops of an aqueous solution of ^{22}NaCl, carrier free, were deposited on a small sheet of the alloy 1.0 cm long x 0.5 cm wide. The water was evaporated up to dryness with the help of an infrared lamp. The final radioactivity deposited on the sheet was about 15 μCi. This sheet was sandwiched by using five other sheets of the same dimensions and covered and fixed with aluminum foil. This arrangement of six sheets and aluminum was put inside a Pyrex tube 8 and 10 mm of internal and external diameters, respectively; this tube was connected to a vacuum system (10^{-4} torr) for 90 minutes to remove the air, and at the end of this evacuation process the 5 cm-long tube was sealed off.

The maximum temperature reached in each thermal treatment was maintained for 20 minutes before cooling the sample. A series of experiments was carried out by using a constant heating rate (CHR) of 3 ± 0.12 K/min.

3. Results and discussion

3.1 PALS

The positron lifetime spectra of the heat-treated alloy were always analyzed by three decaying exponentials from which the lifetimes (τ_1, τ_2, τ_3) and relative intensities (I_1, I_2, I_3) were obtained. Except for the third lifetime component, the rest of the data were temperature dependent.

Each lifetime component is related to a particular annihilation process of positrons in the alloy [8]. For instance, whereas the shortest positron lifetimes, τ_1, are related to the annihilation of positrons in delocalized sites inside the alloy, the intermediate lifetimes, τ_2, are related to the annihilation of positrons inside volumetric defects in the alloy [8. The longest lifetimes with $\tau_3 \sim 1.3$ ns are, on the other hand, related to the annihilation of positronium (Ps) at the surface of the alloy [8], and a low third relative intensity, $I_3 \sim 4\%$ is measured both of which, τ_3 and I_3, remain constant throughout these experiments. These lifetime components give information about the micro-structural changes that the alloy may suffer as a consequence of the thermal treatments. The discussion will, however, be restricted by using the first and second lifetime components only, containing information on the free-volume changes, defect type and other micro-structural changes occurring in the bulk of the alloy [8].

Figure 1 shows the plot of τ_1, v. s. T, where a slight increase in the values of τ_1 is observed from 300 to 550K, the average value being of 147 ps. Then between 611 and 781K the values of τ_1 decrease and fluctuate significantly showing the minimum value of 142 ns at 634K. Notice that these fluctuations on τ_1 appear previous to and at the start of the first crystallization process.

In the crystalline state, the highest value of $\tau_1 = 148$ ps, being obtained from the experimental lifetime data. Since the annihilation site of the first lifetime component arises from delocalized sites, the variation of τ_1 must be associated with atomic rearrangements as already indicated by the MS results. The variations in τ_1 may also arise from volumetric changes in the alloy as will be explained later on.

In this sense, Fig. 2 shows the plot of τ_2 vs T, where large fluctuations on the values of τ_2 also appear, although a slight systematic increase can be observed throughout the entire temperature interval studied.

The magnitudes of τ_2 suggest, on the one hand, the presence of volumetric defects [8], and on the other hand, the fluctuations on τ_2 also suggest that large variations in defect size take place as a consequence of the present heat treatments. Such variations on τ_1 and τ_2 can be further analyzed by their relative intensity variations. For instance, whereas the first relative intensity, I_1, slightly increases, the second one, I_2, slightly decreases, there existing an inverse dependence relation between them (Figs. 3 and 4).

The variations of these two lifetime components are relevant to characterize the defect type that is present in the alloy utilizing the simple trapping model of positrons.

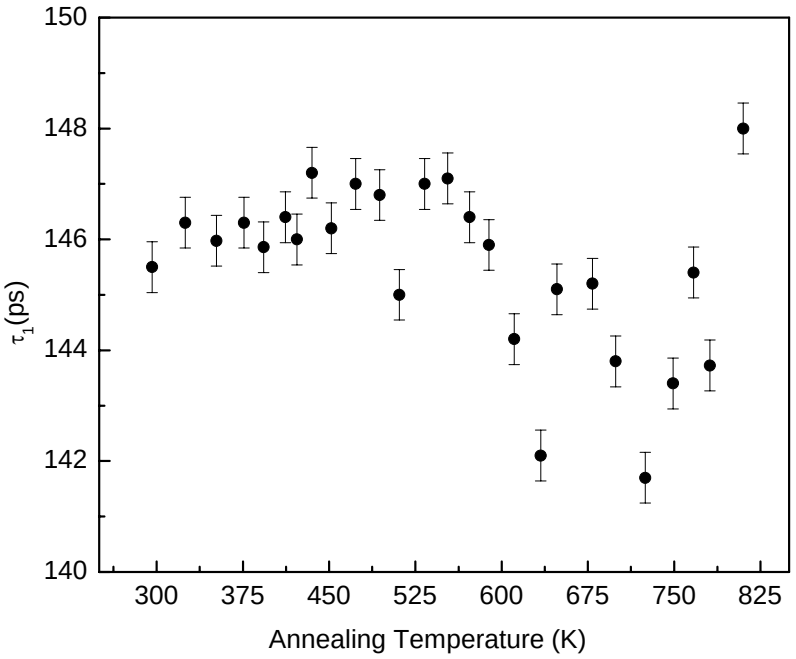

Fig.1. The shortest lifetime, τ_1, alloy measured as a function of annealing temperature in the amorphous and crystalline states of the 2605S3A alloy.

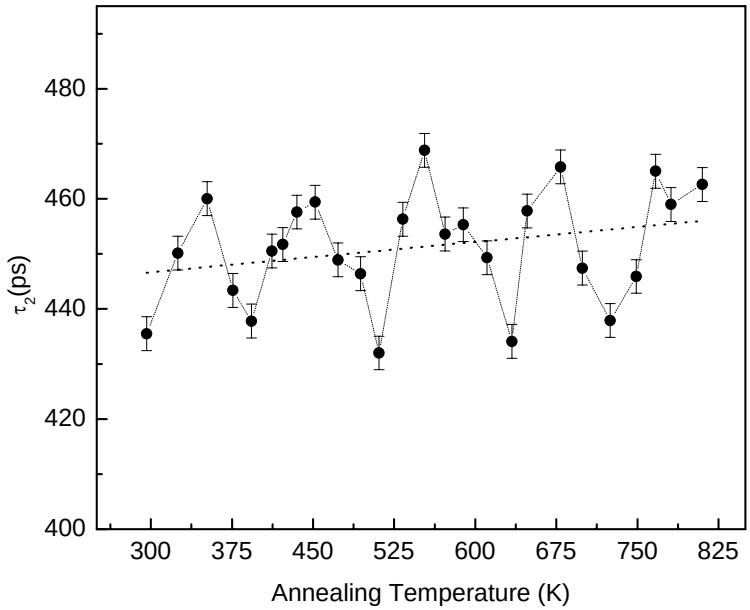

Fig.2. The second lifetime, τ_2, measured as function of annealing temperature in the amorphous and crystalline states of the 2605S3A alloy.

3.2 Defect characterization

In order to remove the third lifetime component from the present analysis, the

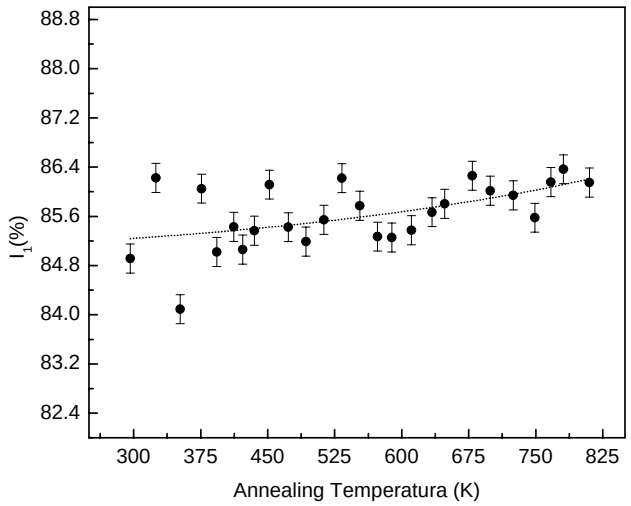

Fig.3. The first relative intensity, I_1, measured as function of annealing temperature in the amorphous and crystalline states of the 2605S3A alloy.

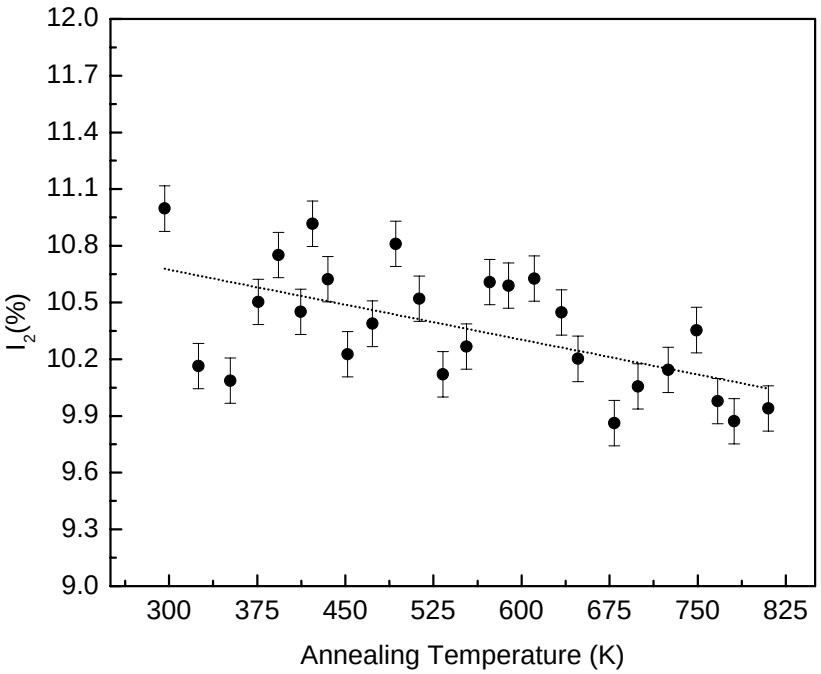

Fig.4. The second relative intensity, I_2, measured as function of annealing temperature in the amorphous and crystalline states of the 2605S3A alloy.

relative intensities I_1 and I_2 must be renormalized according to accepted procedure by using the following formulae:

$$I_1^{\bullet} = \frac{I_1}{I_1 + I_2}, \qquad I_2^{\bullet} = \frac{I_2}{I_1 + I_2}, \tag{1}$$

where the asterisked letters are the renormalized relative intensities [8, 9].

Due to the nature of the PALS data, where the first two lifetime components are temperature dependent only, the simple trapping model of positrons can be used to characterize the volumetric defects in the bulk of the alloy [11]. This model assumes that some positrons annihilate in the bulk of the alloy in a delocalized form with an annihilation rate λ_b [12], with

$$\lambda_b = I_1^{\bullet}\tau_1^{-1} + I_2^{\bullet}\tau_2^{-1}. \tag{2}$$

λ_b being the annihilation rate of positrons in the bulk in the presence of defects. This λ_b has to be differentiated from λ_B, assigned to the annihilation rate constant of positrons in the alloy free of defects [8, 9]. This model also assumes that some other positrons are first trapped in the volumetric defects with a time independent trapping rate constant K [10]. The positrons then eventually annihilate inside the defects with an annihilation rate λ_d [8, 9]. The first lifetime τ_1 turns out to be

$$\tau_1 = \frac{1}{\lambda_b + K}, \tag{3}$$

and the second lifetime is given simply by

$$\tau_2 = \frac{1}{\lambda_d}, \tag{4}$$

where τ_1 and τ_2 are the experimental data. Now the following expressions can be derived from the preceding ones:

$$I_1^{\bullet} = 1 - I_2^{\bullet} \qquad I_2^{\bullet} = \frac{K}{(\lambda_B - \lambda_d + K)} \tag{5}$$

By using Eqs. (5), and leaving K alone, one gets:

$$K = \frac{I_2^{\bullet}}{I_1^{\bullet}}(\lambda_b - \lambda_d), \tag{6}$$

The rate constant K can be estimated from experimental data and can be used to evaluate the defect concentration [10]. Another useful parameter to be handled in this analysis is the mean lifetime of positrons (τ_m)

$$\tau_m = I_1\tau_1 + I_2\tau_2 , \quad (7)$$

giving an estimation of the total free-volume contained in the alloy [7].

On the other hand, Fig. 5 shows the variation of τ_m vs T, where large fluctuations appear, but following practically the same tendency of the τ_1 vs T plot (Fig. 1). In fact every interesting feature of Fig. 1 is enhanced in Fig. 5. For instance, the three minima of τ_m appearing at 511, 634 and 725K are now quite well separated from the rest of the data as compared with the plotted data in Fig. (1). The minimal values of τ_m must be associated with a decreasing of the total free-volume in the alloy [10]. According to present results, the first minimum at 511K is not clearly correlated to any data points of the H_V vs T Fig. 4, Part 1. The next minimum of τ_m appearing at 634K can indeed be related to the H_V Fig. 4, Part 1. For instance, at 634K the brittleness of the alloy begins, as already discussed in the H_v section. This premature change on this mechanical property in the amorphous state of the alloy should then be associated with a decrease of the

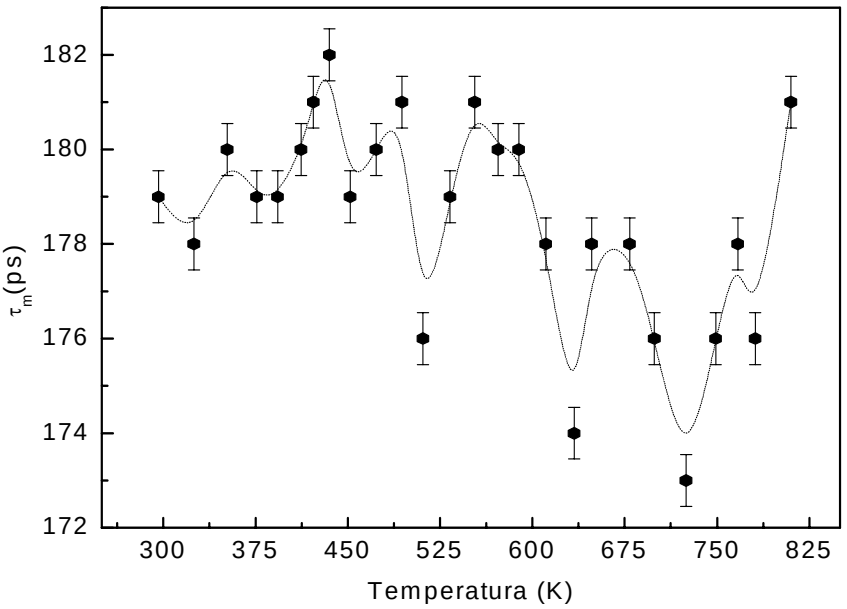

Fig.5. Mean lifetime of positrons in the amorphous and crystalline states of the 2605S3A alloy given as function of the annealing temperature.

free-volume in the alloy rather than to be associated with the presence of crystalline material. The expected value of B_{hf} at 634K could be about 23.77 T, having taken this value as the average value between the B_{hf} values recorded at 601 and 648K. This value of 23.77T is slightly higher than that measured for the untreated alloy with B_{hf} = 23.05 T. Thus, the reduction of free-volume in the sample at 634K is related to a shortening of the Fe-Fe distances and this is probably the cause of the premature brittleness problem of the alloy. The third minimum of τ_m appearing at 725K is clearly correlated to the large increase of the Vickers number, H_V = 10.75 GPa, associated with the high degree of brittleness in the alloy Fig. 4, Part 1. Although the Mössbauer spectrum was not recorded after treating the alloy at 725K the tendency of the data in Fig. 7, Part 1 indicates that the hyperfine magnetic field decreases and a magnetic reorientation sets in, respectively. Notice from Fig. 7 that intensities of peaks 2 and 5 decreased after treating the sample at 749K. It is to be noticed from Figs. 5 and 7, Part 1 that since the alloy still remained in its amorphous state after treating it at 725, the brittleness property of the alloy should still be associated with the decrease of free-volume rather than to the presence of crystalline phases which are not present at this point of the thermal treatments. Other studies have shown that in some alloys the formation of dendrites, the precursors of crystalline material, appear before subjecting to alloy to the phase transitions temperatures, T_g and T_x [6]. The presence of these dendrites could also be an additional source of the brittleness problem of the present alloy.

3.3 The electronic densities in the bulk and defects

Connected with these micro-structural changes in the alloy, the electronic density in the bulk and surrounding the defects can also be estimated from

$$N_i = \frac{(\lambda_i - 2)}{134} \text{ (a. u.) with i = b or d,} \qquad (8)$$

where b and d refer to bulk and defect, respectively [11]. Experimental results show that both the N_b and N_d present maximal values at 511, 634 and 725K suggesting that electronic changes in the bulk and around the defects are also involved, changing the mechanical and magnetic properties of the alloy. Also from same results, the values of N_d are of one order of magnitude lower than those of N_b, suggesting an amount of electronic charge in the defect lower than that in the bulk. This difference between n_d and n_b is an additional suggestion that the annihilation site of the second lifetime component should consist of volumetric defects rather than of mass defects.

3.4 Defects concentration and size

Before considering the size and type of these volumetric defects, let us introduce the concentration C concept [11]

$$C = \frac{K}{\mu} = \frac{K}{N\nu}. \quad (9)$$

As an approximation

$$\mu \approx 2.98148x10^{16}\ s^{-1}. \quad (10)$$

This value of $\mu = N\nu$ value was obtained as follows: N represents the atomic density and ν the specific trapping rate of positrons whose values are [11]:

$$N = 0.602x10^{24}\left(\frac{d}{A}\right)\ (cm^{-3}), \quad \nu = 4\pi R_d D_+\ (cm^3/s) \quad (11)$$

The density of the alloy is d = 7.29 g/cm^3 (Metglass Inc. Co.). The atomic number of the alloy was taken as a weighted value, estimated from the elemental analysis results given by PIXE: $Fe_{95.30}Cr_{2.46}Mn_{0.14}Si_{0.90}$. From this, A = 55.499 a. m. u. The values of the defect radius R_d and diffusion coefficient D_+ are usually unknown parameters. In this sense R_d can be expressed in terms of the Wigner-Zeits unit cell radius r_s assuming a spherical packing [15].

$$R_d = \sqrt[3]{N_V Z} r_s, \quad (12)$$

where N_V is the number of vacancies in the volumetric defect and Z = 2.1248 is the weighted valence electron obtained from the elemental formula $Fe_{95.30}Cr_{2.46}Mn_{0.14}Si_{0.90}$. The radius r_s can be estimated from [10]

$$r_s = 1.389\sqrt[3]{\frac{A}{Zd}}. \quad (13)$$

As an approximation to the actual diffusion coefficient D_+ in the alloy, the following was considered. The mean free path of positrons in metals is $L_+ \approx 10^3$ Å [15, 16]. Since L_+ can be expressed by [17]

$$L_+ \approx \sqrt{D_+ \tau_c}, \quad (14)$$

with τ_c = 146 ps being the average lifetime of positrons in the alloy estimated from all first lifetimes obtained. Taking these considerations into account, a diffusion coefficient for the present alloy could be $D_+ = 0.684931 cm^2/s$.

3.5 Defect type

In order to determine the parameter N_V involved in Eq. (20) it is necessary to refer to the work of Puska and Nieminen [18] who theoretically determined the annihilation rates of positrons in volumetric defects contained in metals. In their paper, volumetric defects (clusters of mono-vacancies) of different shapes and sizes were simulated [18]. The data correlating the lifetimes of positrons and these clusters in metallic Fe will, therefore, be used to grossly characterize the type of defects in the amorphous and crystalline alloy, which contains about 95.30 W% of Fe. Figure 8 shows such a correlation. The dotted points in Fig. 8 represent the theoretical correlation between the positron lifetime and the characteristics of the cluster of vacancies [18].

The second lifetimes founded lie within those reported in Fig. 6. The dash in Fig. 6 represents the fitting of the data by using the following Pade function [19]

$$f(x) = \frac{a + bx}{c + dx}. \qquad (15)$$

The resulting coefficients were a = 567.51203, b = 208.88855, c = 4.23997 and d = 0.35559.

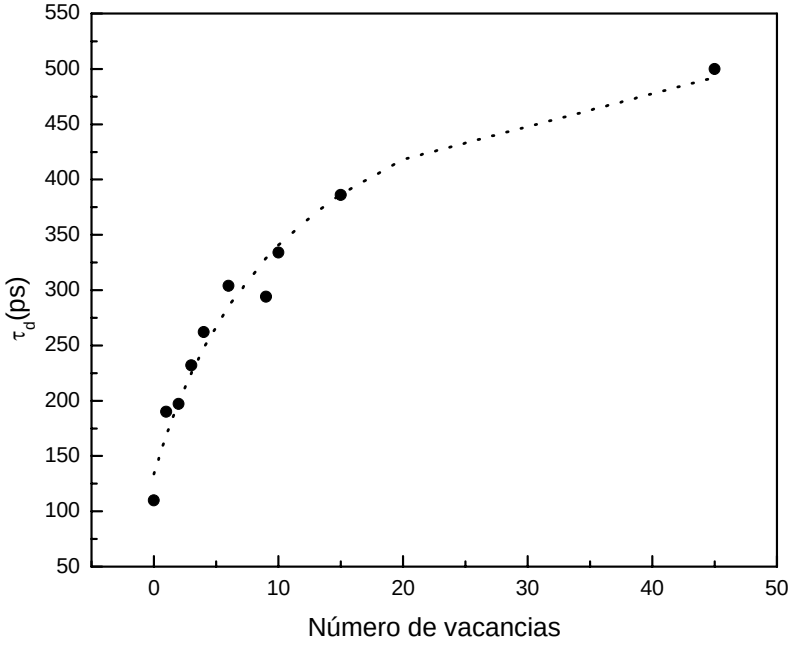

Fig.6. Number of vacancies vs the positron lifetime. The thin dotted line represents the fitting of the theoretical data of Puska and Nieminen [Ref] for pure Fe. The fitting was done by using a Padé function as described in the text.

As expected, at 511, 634 and 725K, the smallest clusters of vacancies were obtained with a mean radius of R_d = 0.413 nm.

It can be finally observed from Fig. 7 that at these temperatures the concentrations of defects are also maximal. One may notice from Fig. 7 the oscillatory nature of the data between 452 and 810K. This oscillatory tendency of the data remains to be investigated in order to correlate it fully with the observed change of properties occurred in the alloy.

Finally, with the experimental data, it is now possible to grossly estimate the concentration of defects at each thermal treatment, which includes the type of defect and the defect radius. An average value for the concentration of defects between the amorphous and crystalline state was C = 1.68×10^{-8} at^{-1}, a value that is characteristic in metals and alloys.

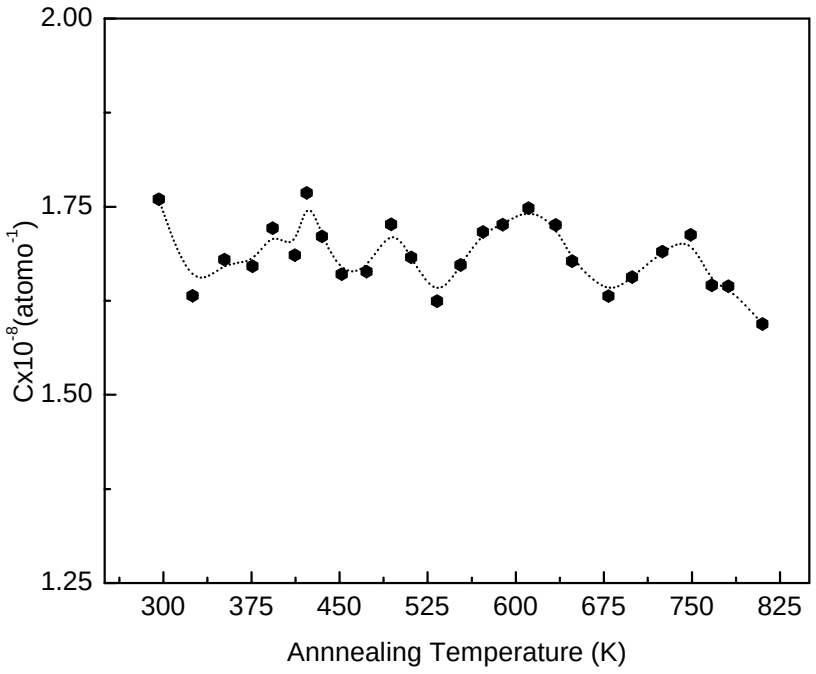

Fig.7. Relative concentration of defects measured as function of annealing temperature in the amorphous and crystalline states of the 2605S3A alloy.

4. Conclusions

A micro-structural analysis was made in the heat treated amorphous alloy 2605S3A by studing the presence of volumetric defects as detected by PALS and their connection with the magnetic reorientations that took place either in the amorphous state or previous to the crystallization process. The detected volumetric defects, consisting of clusters of vacancies ranging between 24 and 32 vacancies, had a mean average radius and mean relative concentration of 0.44 nm and C = $1.68x10^{-8}$ at^{-1}, respectively. The variations of R_d and C were shown to be important factors to promote the deterioration of the ductility of the alloy previous to the crystallization process. Moreover, our studies show that, as a result of several times heat treating of the present alloy below the phase transition temperatures T_g and T_x, the formation of other crystalline phases, different from pure Fe, could be inhibited. These results will be further investigated meticulously by using MS and XRD to fully establish the effects on the alloy physical properties. More experimental data are needed to see, whether the PALS and Mössbauer results completely match as suggested by the present results.

Acknowledgments. We are grateful to J. Jordan and Dr. Hasegawa from Metglass Inc. Co. in the USA for providing us the alloy 2605S3A subject of this study. We also appreciate the technical support of the Laboratory of Materials at ININ for the H_V measurements.

Bibliography

[1] Brener, A.; Riddell, G.E.: Nickel Plating on Steel by Chemical Reduction. J. of Research of the National Bureau of Standards, 37, 31 (1946)

[2] Yoshimi Makino: The application of non-crystalline materials in Japan. Current Topic on non-crystalline solids, edited by Boro, M.D.; Clavaguerra, N. 87 (1986)

[3] Nosenko, V.K.; Maslov, V.V.; Kirilchuk, V.V.; Kochkubey, A.P.: Some industrial applications of amorphous and nano-crystalline alloys. Journal of Phys.: Conference Series 98, 1 (2008)

[4] Cabral-Prieto, A.; Garcìa-Santibàñez, F.; Lòpez, A., Lòpez-Castañares, R.; Olea-Cardoso, O.: Vickers Microhardness and Hyperfine Magnetic Field Variations of Heat Treated Amorphous $Fe_{78}Si_9B_{13}$ Alloy Ribbons. Hyperfine Interactions **161**, 69 (2005)

[5] Allia, P.; Tiberto, P.; Baricco, M.: Vinai, F.: Improved ductility of nano-crystalline $Fe_{73.5}Nb_3Cu_1Si_{13.5}B_9$ obtained by direct-current joule heating, Appl. Phys. Lett., **83** (20), 2759 (1993)

[6] Bang, T.Y.; Lee R.Y.: Crystallization of the metallic glass $Fe_{78}Si_9B_{13}$, J. Mater. Sc. **26**, 4961 (1991)

[7] Linderoth, S.; Gonzalez, J. M.; Hidalgo, C.; Liniers, M.; Vincent, J. L. ;: Correlation between positron lifetime results and magnetic behavior upon relaxation and crystallization of an iron-based amorphous alloy. Solid State Commun. **65** (12), 1457(1988)

[8] Hautojarvy, P. Positrons in Solids, Topics in Current Physics, No 12, 1979 Edited by Hautojarvy, P.: Springer-Verlag, Berlin Heidelberg New York. Chapter 1, 1-22.

[9] Hautojarvy, P.; Corbel, C.: Positron Spectroscopy of Defects in Metals and Semiconductors, Positron Spectroscopy of Solids. Editado por Dupasquier and A.P. Mills Jr., 491 (1995)

[10] Eldrup, M.: Application of the positron annihilation technique in studies of defects in solids, Defects in Solids 1986, Edited by Chadwick, A.V.; Trenzi. M. Chapter 2**,** 145-178.

[11] Brandt, W., Positron Dynamics in Solids, Applied Physics, **5**, 1 (1974)

[12] Mössbauer Spectroscopy (1975), edited by U. Gonser, Springer-Verlag Berlin**,** Chapter 1,1-51

[13] Kirkgaard, P. and Eldrup, M. Comput. Phys. Commun. **3**, 240 (1972)

[14] Hautojarvy, P., Heinio, J., Manninen, M.; Nieminen, R.: 1977, Philosophical

Magazine, **35** (4), 937 (1977)

[15] Particle Induced X-Ray Emission Analysis. Application to Analytical Problems, 1981. Edited by Zucker, A.: Oak Ridge National Laboratory

[15] Paulin, R.; Ripon, R.; Brandt, W.: Diffusion Constant and Surface States of Positrons in Metals, Applied. Physics **4**, 343 (1974)

[16] Schultz, P.J.; Lynn, K.G.: Rev. Mod. Phys., **60,701** (1988)

[17] J, Cizek, J.; Prochazka, I.; Kmjec, T.; Vostry, P.: Using of Modified trapping model in Positron-lifetime study of cold-worked aluminium, Phys. Stat. Sol. (a) **180,** 439 (2000)

[18] Puska, M.J.; Nieminen, R. M.: Defect spectroscopy with positrons: a general calculation method. J. Phys. F: Met. Phys, **13**, 333 (1983)

[19] Burden, R. I.; Faires, J. D.: Análisis Numérico, Iberoamericana, Chapter 10, 427 (1985).